



*Supplement of*

## **Anthropogenic aerosol forcing of the Atlantic meridional overturning circulation and the associated mechanisms in CMIP6 models**

**Taufiq Hassan et al.**

*Correspondence to:* Robert J. Allen ([rjallen@ucr.edu](mailto:rjallen@ucr.edu)) and Taufiq Hassan ([mhass004@ucr.edu](mailto:mhass004@ucr.edu))

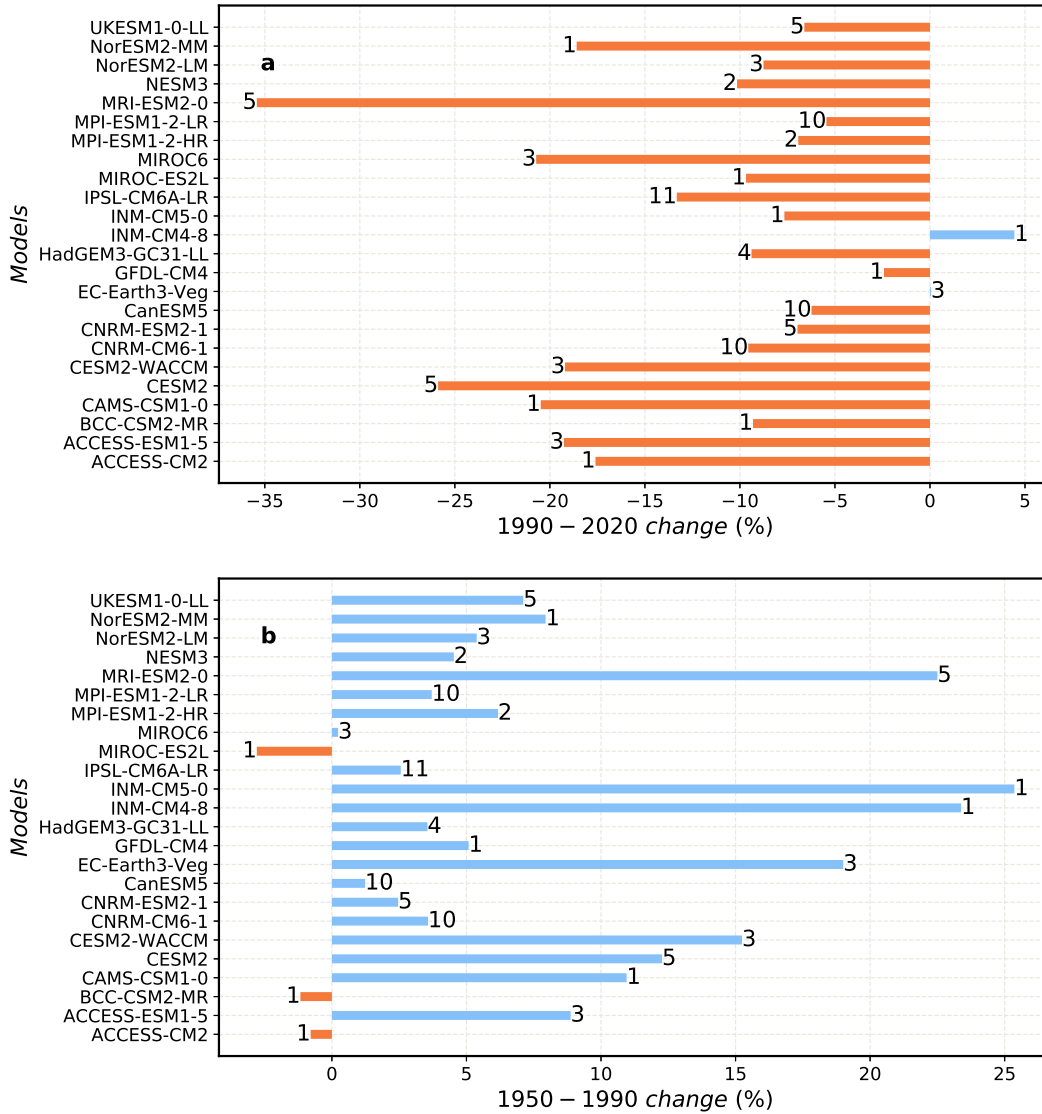
The copyright of individual parts of the supplement might differ from the article licence.

**SUPPLEMENTARY TABLE 1 Present-day (2005-2018) climatological AMOC strength based on RAPID observations and Coupled Model Intercomparison Project phase 6 all forcing models.** The AMOC is defined as the maximum stream function below 500 m in the Atlantic. AMOC units are Sverdrups (Sv), where 1 Sv is equal to  $10^6 \text{ m}^3 \text{ s}^{-1}$ .

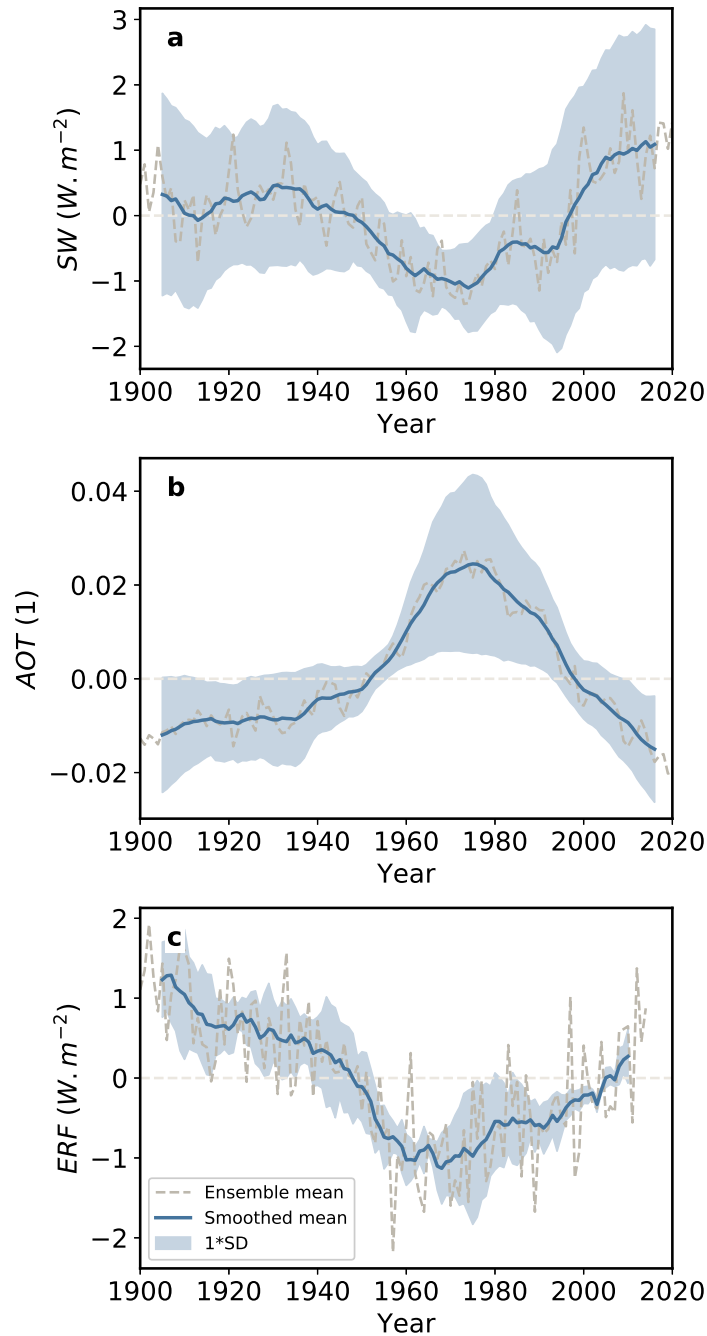
Model	AMOC Mean (Sv)
CAMS-CSM1-0	13.0
MPI-ESM1-2-HR	29.1
ACCESS-CM2	18.8
NESM3	9.1
MIROC6	18.1
CESM2	22.0
MPI-ESM1-2-LR	25.3
IPSL-CM6A-LR	11.6
CNRM-CM6-1	15.4
MIROC-ES2L	18.8
HadGEM3-GC31-LL	16.8
ACCESS-ESM1-5	20.3
CESM2-WACCM	22.8
BCC-CSM2-MR	25.4
INM-CM5-0	18.3
NorESM2-MM	30.3
CNRM-ESM2-1	15.4
INM-CM4-8	25.4
NorESM2-LM	28.3
MRI-ESM2-0	18.6
EC-Earth3-Veg	17.0
UKESM1-0-LL	17.0
GFDL-CM4	21.8
CanESM5	13.1
RAPID	17.5

SUPPLEMENTARY TABLE 2 **Anthropogenic aerosol Effective Radiative Forcing (ERF) and AMOC percent change in CMIP6 models.** Aerosol ERF is calculated for the globe (GL), Europe (EU; 30-45°N; 0-30°E) and the subpolar North Atlantic (sNA; 45-60°N; 0-50°W). AMOC percent change is shown for both time periods, 1950-1990 and 1990-2020. Aerosol ERF is calculated as the net TOA radiative flux difference between piClim-Control and piClim-aer simulations (i.e., piClim-aer–piClim-Control). Models are arranged from largest (absolute value) global mean aerosol ERF to lowest. Aerosol ERF units are  $\text{W m}^{-2}$  and AMOC percent change units are %.

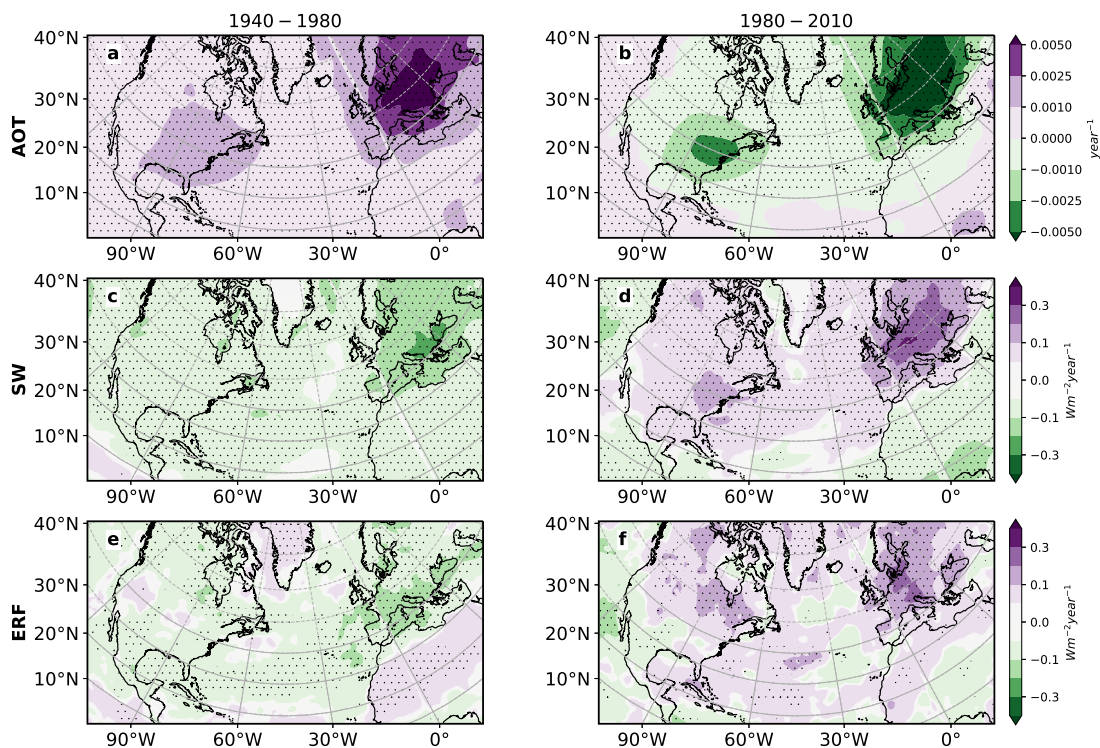
Model	Aerosol ERF			AMOC	
	GL	sNA	EU	1950-1990	1990-2020
NorESM2-LM	-1.31	-2.35	-0.70	4.9	-8.1
NorESM2-MM	-1.26	-2.22	-0.72	8.9	-15.7
MRI-ESM2-0	-1.19	-0.22	-2.56	21.8	-29.6
CNRM-CM6-1	-1.15	0.26	-1.48	3.3	-9.0
UKESM1-0-LL	-1.11	-2.01	-0.79	6.8	-6.2
HadGEM3-GC31-LL	-1.10	-1.24	-0.96	3.3	-8.5
MIROC6	-1.04	-0.64	-1.06	0.1	-20.9
CanESM5	-0.85	-2.20	-1.07	0.7	-5.5
CNRM-ESM2-1	-0.74	0.23	-1.08	2.6	-7.2
GFDL-CM4	-0.73	-0.76	-1.20	3.1	-2.3
CESM2	-0.65	-0.38	-0.09	11.3	-23.9
IPSL-CM6A-LR	-0.64	-0.14	-1.39	1.9	-12.9



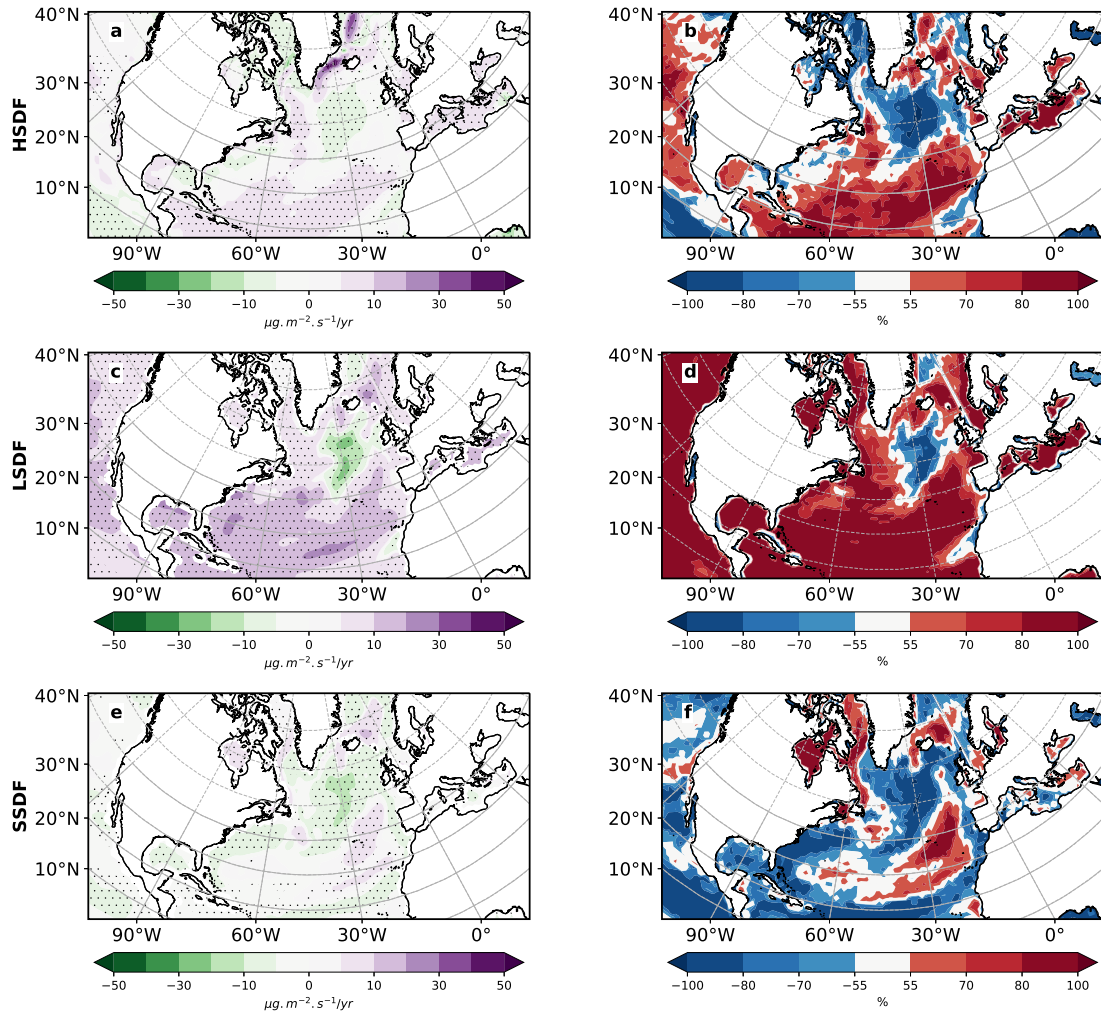
**SUPPLEMENTARY FIGURE 1 Ensemble mean AMOC percent change in all forcing Coupled Model Intercomparison Project phase 6 models.** Ensemble mean (a) 1990-2020 and (b) 1950-1990 AMOC percent change [%] for each model. AMOC weakening (strengthening) is shown with orange (blue) bars. Numbers in front of each bar represent the number of simulations used for that model. The AMOC percent change is estimated from the least-squares regression slope ( $r_s$ ) of the non-normalized AMOC time series using:  $100 \times \frac{r_s \times N}{AMOC(N=1)}$ , where  $N$  is the number of years (e.g., 30 for 1990-2020) and  $AMOC(N=1)$  is the initial AMOC strength (e.g., in 1990 for 1990-2020).



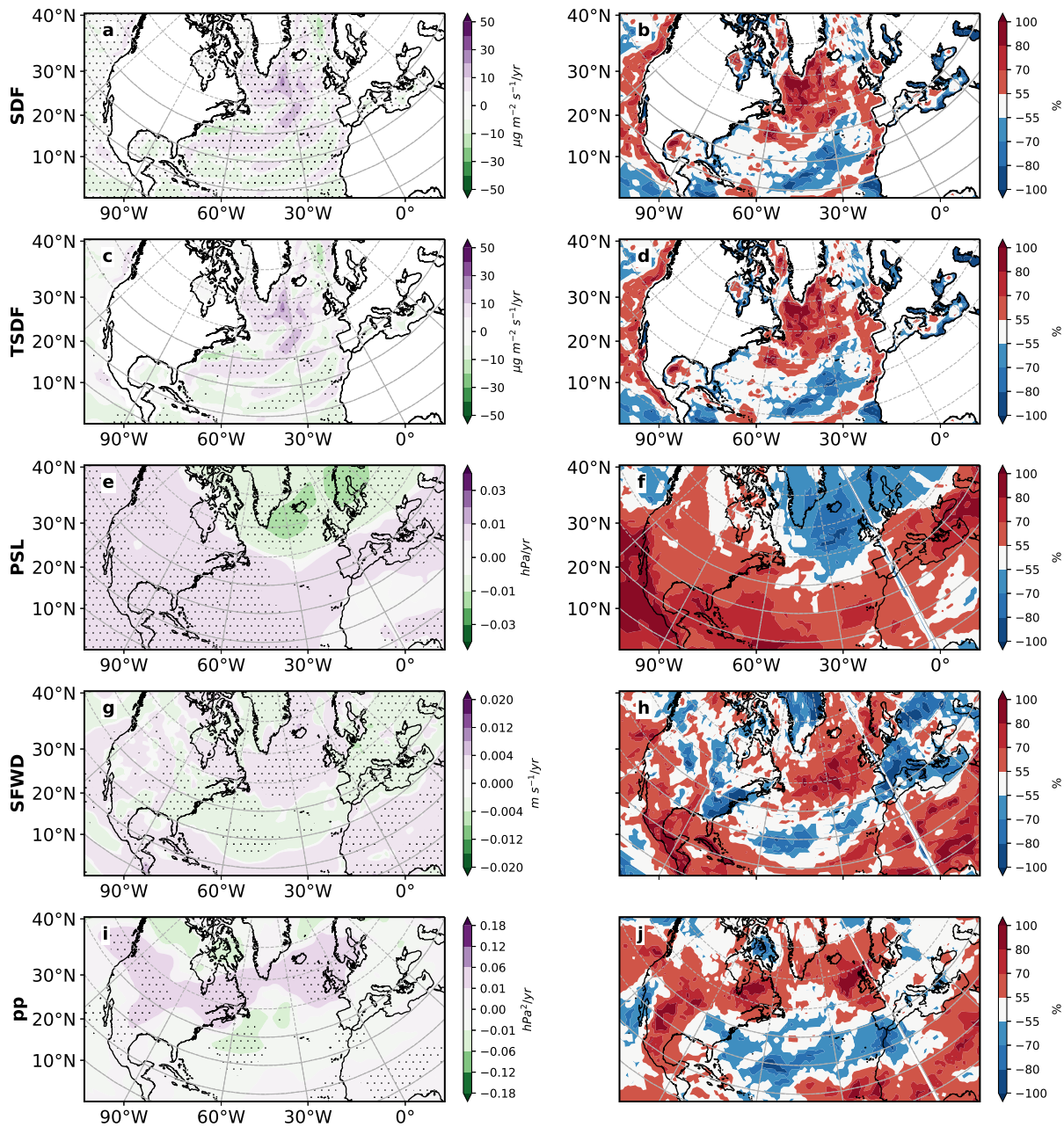
**SUPPLEMENTARY FIGURE 2 1900-2020 ensemble mean annual mean Coupled Model Intercomparison Project phase 6 normalized time series.** (a) net downward surface shortwave radiation (SW); (b) 550 nm aerosol optical thickness (AOT); and (c) anthropogenic aerosol effective radiative forcing (ERF). SW and AOT are based on CMIP6 anthropogenic aerosol forcing simulations. ERF is calculated from the histSST and histSST-piAer experiments, using the net top-of-the-atmosphere radiative flux. Only three models are available for the aerosol ERF calculation, including MIROC6, UKESM1-0-LL, and NorESM2-LM, and these simulations end in 2014. Values are averaged over the subpolar North Atlantic ( $45^{\circ}\text{N}$  to  $60^{\circ}\text{N}$  and  $0^{\circ}\text{W}$  to  $50^{\circ}\text{W}$ ). The ensemble mean time series (gray dashed) is smoothed using a 10-year running mean (solid blue line). Shading shows the corresponding inter-model standard deviation. Each model is normalized by its long-term (1900-2020) climatology. Units for SW and ERF are  $\text{W m}^{-2}$ . AOT is dimensionless.



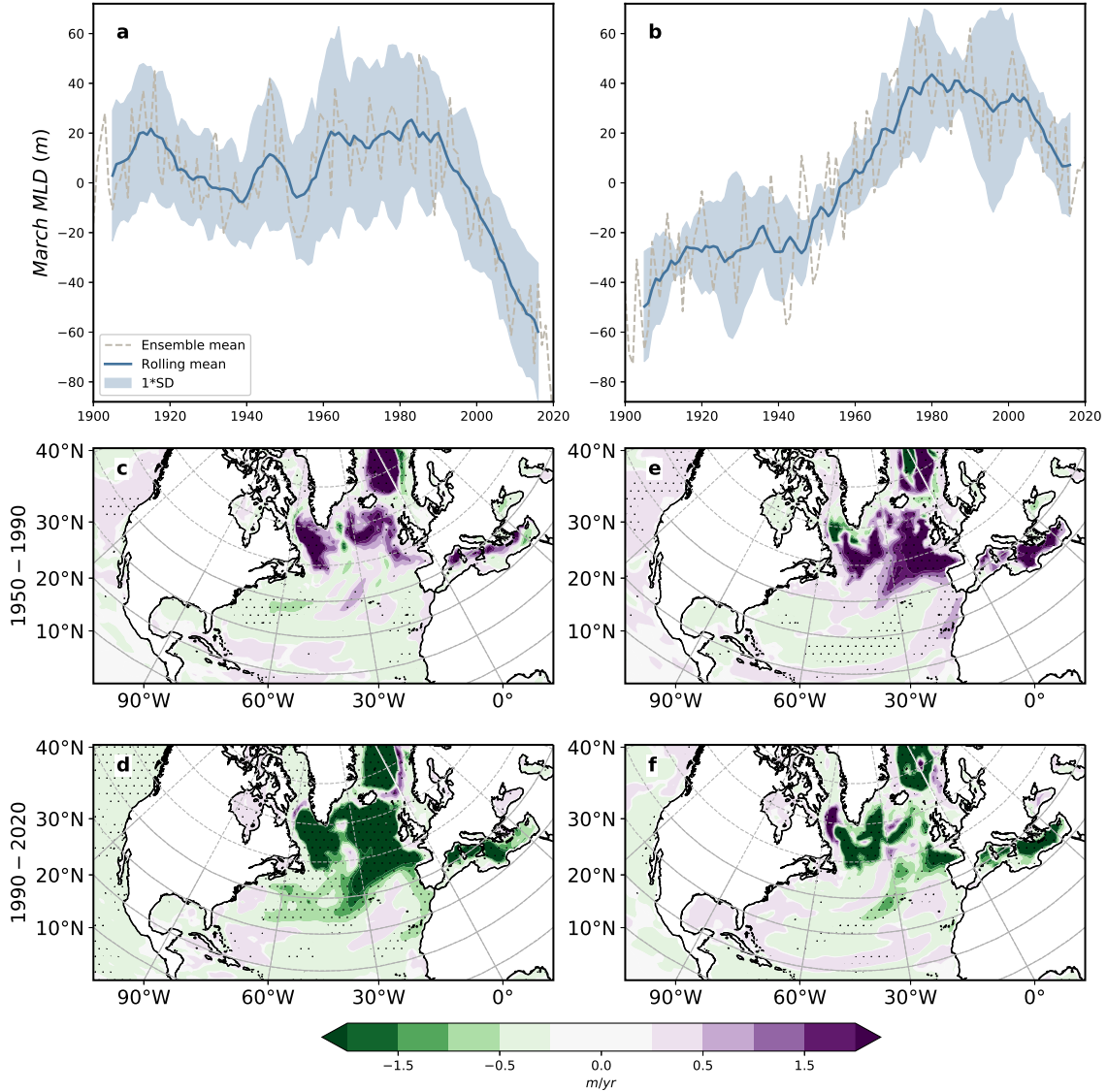
**SUPPLEMENTARY FIGURE 3 Ensemble mean annual mean Coupled Model Inter-comparison Project phase 6 trends.** (left panels) 1940-1980 and (right panels) 1980-2010 (a-b) 550 nm aerosol optical thickness (AOT); (c-d) net downward surface shortwave radiation (SW); and (e-f) anthropogenic aerosol effective radiative forcing (ERF). Trends here have been shifted by 10 years earlier, due to the  $\sim 10$  year lead correlation with the AMOC. SW and AOT are based on CMIP6 anthropogenic aerosol forcing simulations. ERF is calculated from the histSST and histSST-piAer experiments, using the net top-of-the-atmosphere radiative flux. Only three models are available for the aerosol ERF calculation, including including MIROC6, UKESM1-0-LL, and NorESM2-LM. Symbols designate trend significance at the 95% confidence level based on a *t*-test. Trend units for AOT are year<sup>-1</sup> and W m<sup>-2</sup> year<sup>-1</sup> for SW and ERF.



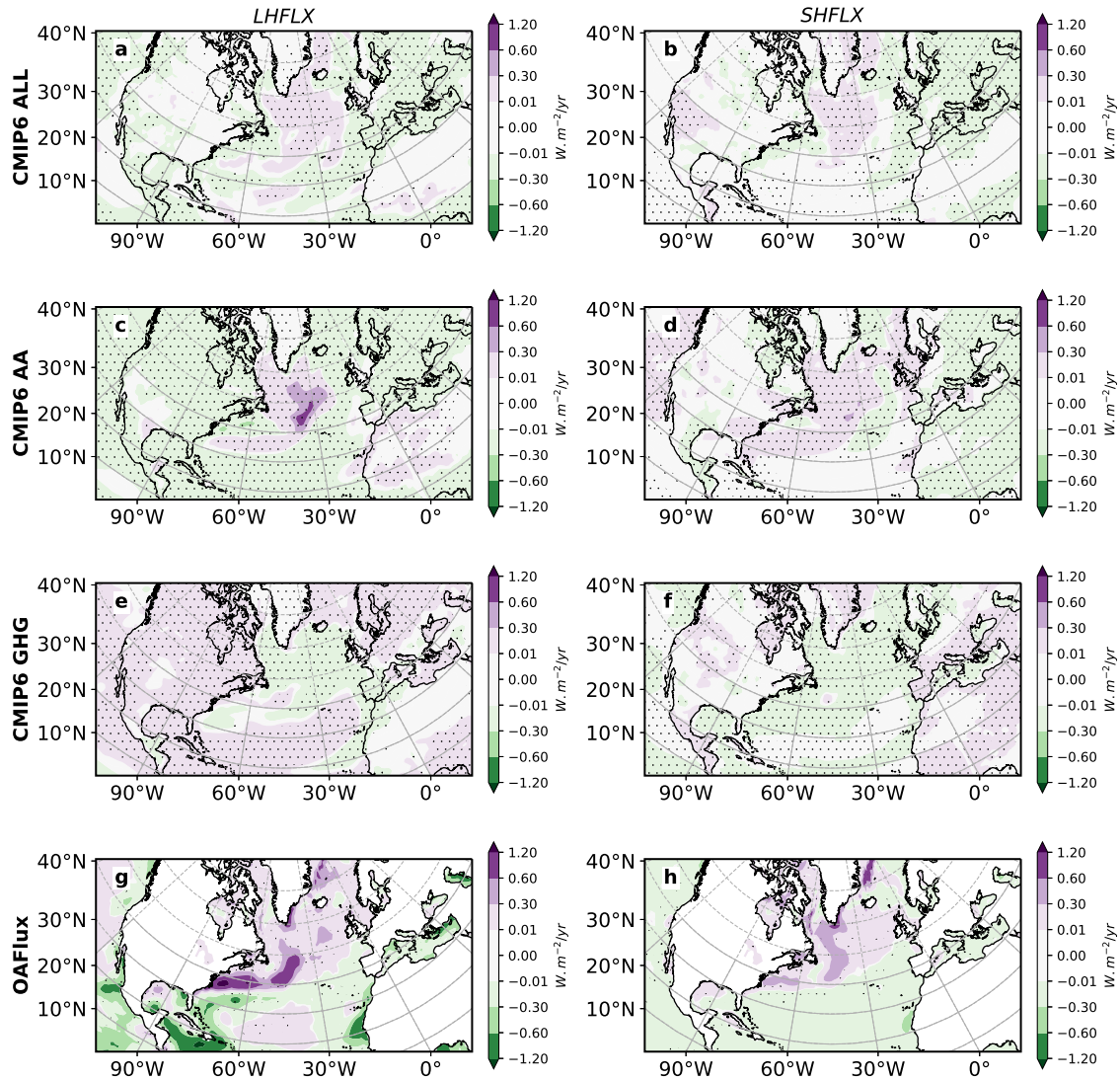
**SUPPLEMENTARY FIGURE 4 1990-2020 annual mean all forcing Coupled Model Intercomparison Project phase 6 ensemble mean trends and model agreement on the sign of the trend.** (a-b) haline surface density flux (HSDF); (c-d) latent heat induced surface density flux (LSDF); and (e-f) sensible heat induced surface density flux (SSDF). Left panels show the ensemble mean trend; right panels show model agreement on the sign of the trend for each model's ensemble mean. Symbols in left panels designate trend significance at the 95% confidence level based on a  $t$ -test. Trend units are  $\frac{\mu\text{g}}{\text{m}^2\text{-s}} \text{ year}^{-1}$ . Trend realization agreement units are %. Red (blue) colors indicate model agreement on a positive (negative) trend.



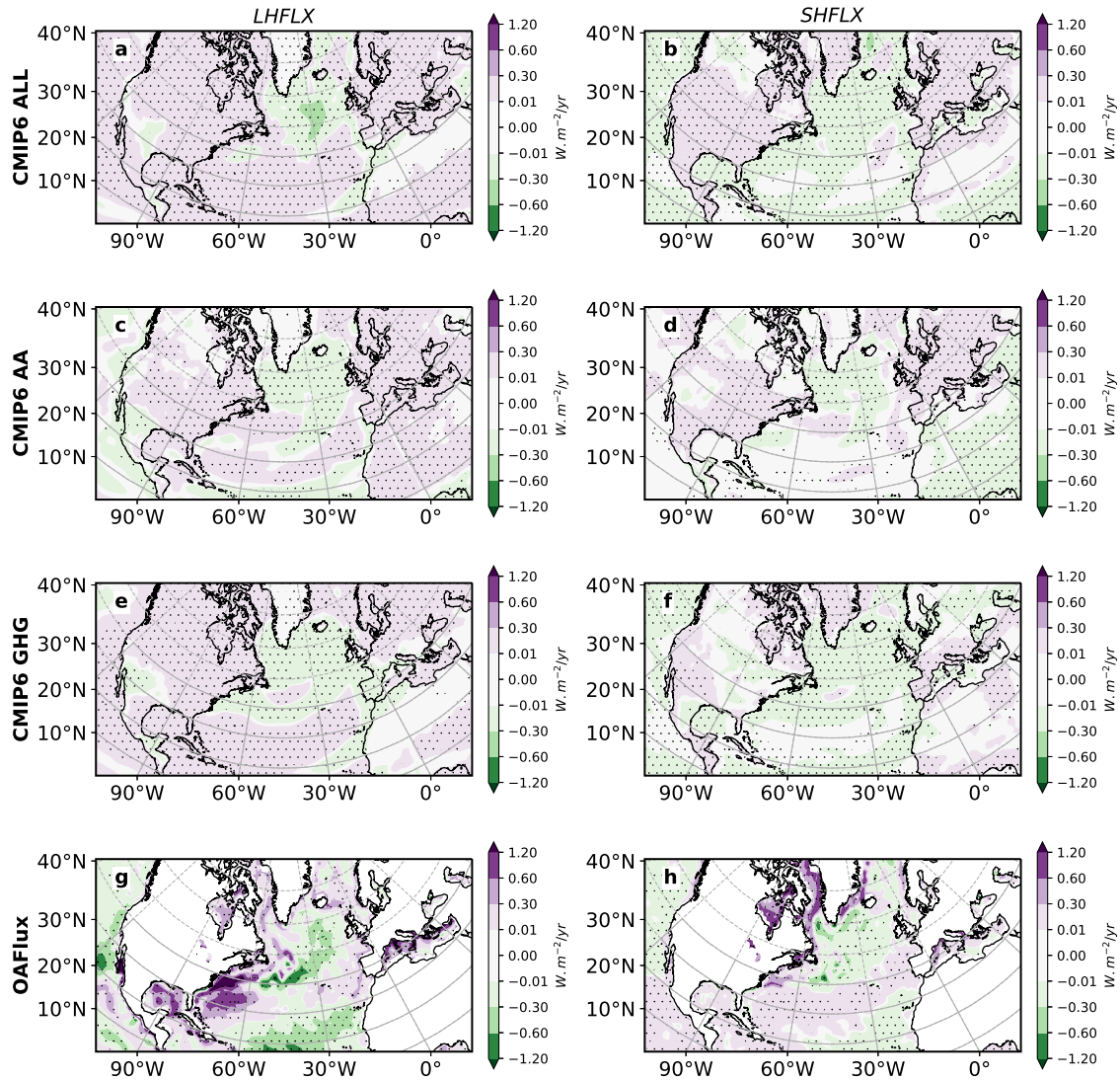
**SUPPLEMENTARY FIGURE 5 1950-1990 annual mean all forcing Coupled Model Intercomparison Project phase 6 ensemble mean trends and model agreement on the sign of the trend.** (a-b) surface density flux (SDF); (c-d) thermal SDF (TSDF); (e-f) sea level pressure (PSL); (g-h) surface winds (SFWD); and (i-j) storm track activity (pp). Left panels show the ensemble mean trend; right panels show model agreement on the sign of the trend for each model's ensemble mean. Symbols in left panels designate trend significance at the 95% confidence level based on a  $t$ -test. SDF and TSDF trend units are  $\frac{\mu\text{g}}{\text{m}^2\text{-s}} \text{ year}^{-1}$ . PSL, pp, and SFWD trend units are  $\text{hPa year}^{-1}$ ,  $\text{hPa}^2 \text{ year}^{-1}$ , and  $\text{m s}^{-1} \text{ year}^{-1}$ , respectively. Trend realization agreement units are %. Red (blue) colors indicate model agreement on a positive (negative) trend.



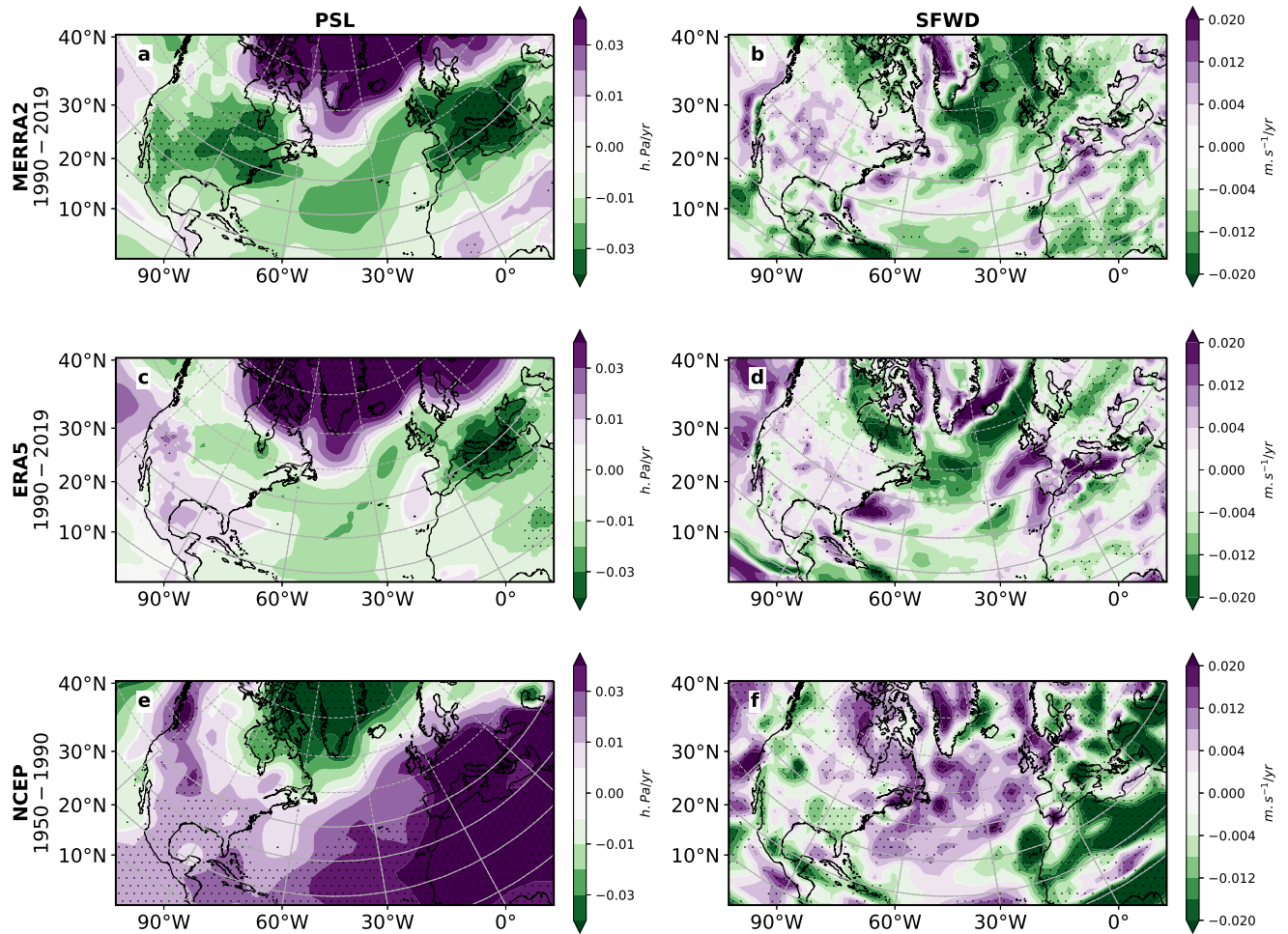
**SUPPLEMENTARY FIGURE 6 Ensemble mean annual mean Coupled Model Inter-comparison Project phase 6 time series and trends.** (a, c, d) all forcing and (b, e, f) anthropogenic aerosol forcing March Mixed Layer Depth (MMLD). (a, b) subpolar North Atlantic time series; (c, e) 1950-1990 trend maps and (d, f) 1990-2020 trend maps. The ensemble mean time series (gray dashed) is smoothed using a 10-year running mean (solid blue line). Shading shows the corresponding inter-model standard deviation. Each model is normalized by subtracting its long-term (1900-2020) climatology. Symbols in bottom panels designate trend significance at 95% confidence level based on a t-test. MMLD trend units are in m/year.



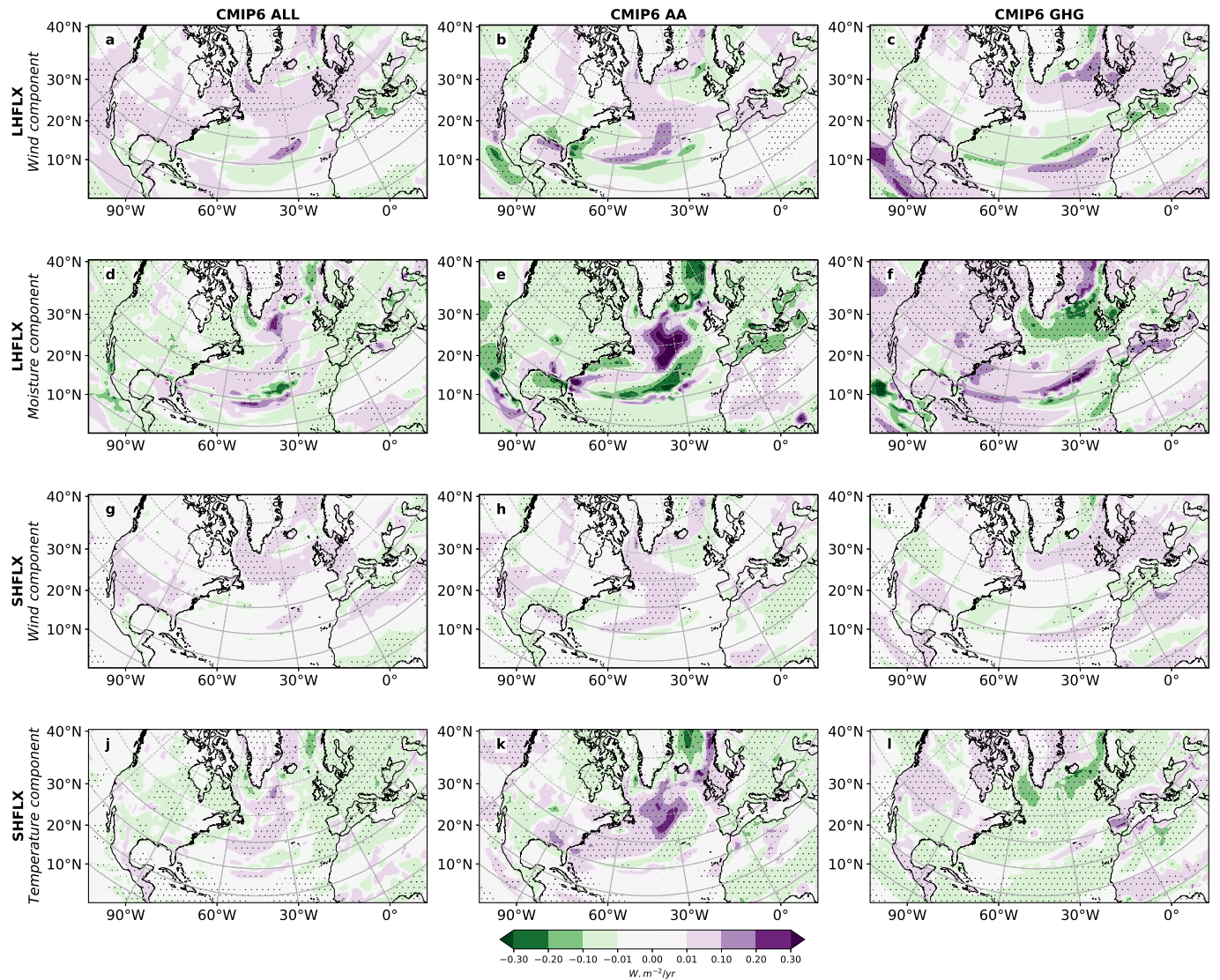
**SUPPLEMENTARY FIGURE 7 Annual mean Coupled Model Intercomparison Project phase 6 ensemble mean and observed heat flux trends.** 1950-1990 CMIP6 ensemble mean (top panels) all forcing (a) latent heat flux (LHFLX) and (b) sensible heat flux (SHFLX) trends; (top middle panels) anthropogenic aerosol (AA) forcing (c) LHFLX and (d) SHFLX trends; and (bottom middle panels) greenhouse gas (GHG) forcing (e) LHFLX and (f) SHFLX trends. 1958-1990 (bottom panels) Objectively Analyzed air-sea Fluxes (OAFflux) (g) LHFLX and (h) SHFLX trends. Symbols in panels designate trend significance at the 95% confidence level based on a  $t$ -test. Trend units are  $\text{W m}^{-2} \text{ year}^{-1}$ .



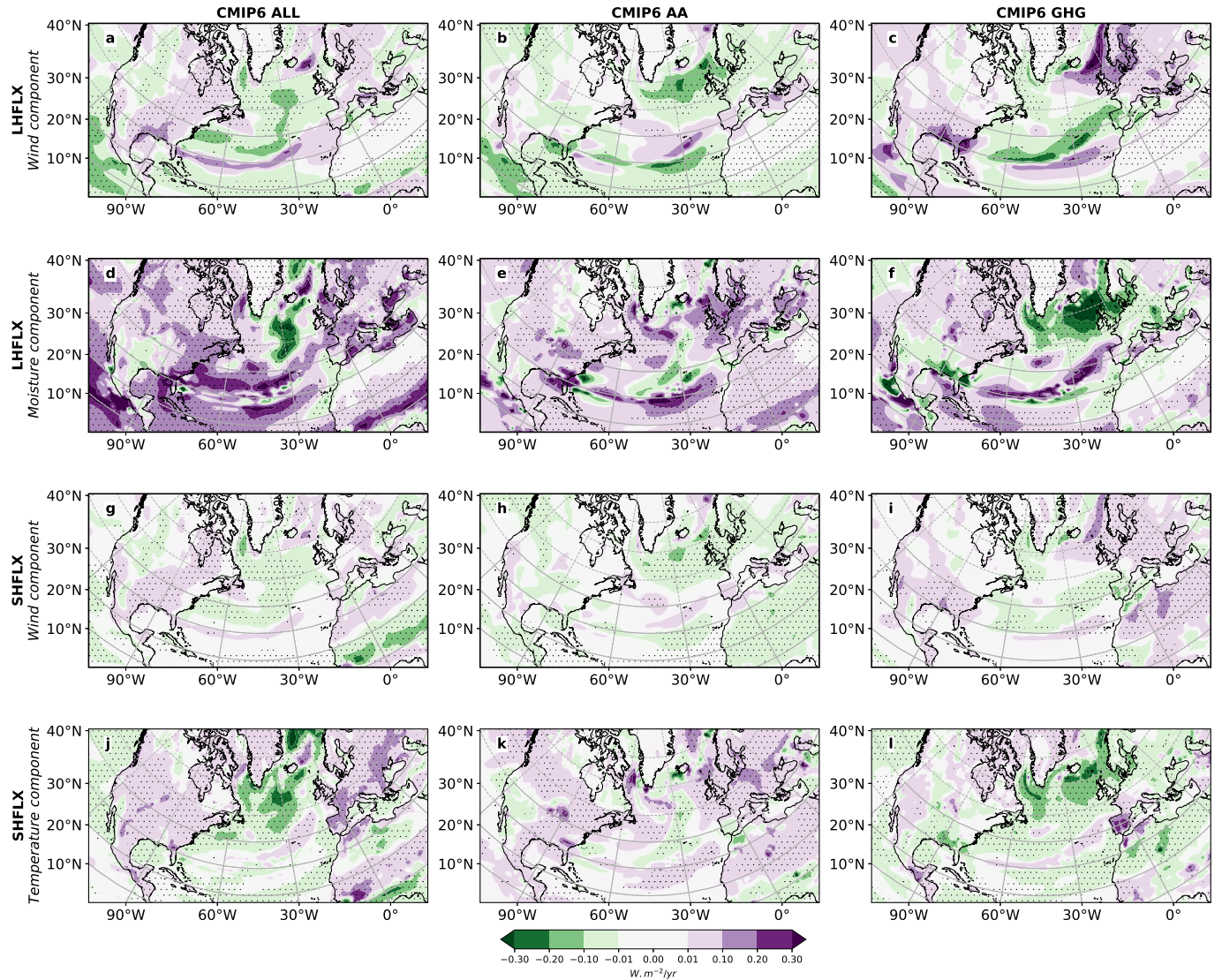
SUPPLEMENTARY FIGURE 8 **Annual mean Coupled Model Intercomparison Project phase 6 ensemble mean and observed heat flux trends.** 1990-2020 CMIP6 ensemble mean (top panels) all forcing (a) latent heat flux (LHFLX) and (b) sensible heat flux (SHFLX) trends; (top middle panels) anthropogenic aerosol (AA) forcing (c) LHFLX and (d) SHFLX trends; and (bottom middle panels) greenhouse gas (GHG) forcing (e) LHFLX and (f) SHFLX trends. 1990-2018 (bottom panels) Objectively Analyzed air-sea Fluxes (OAFflux) (g) LHFLX and (h) SHFLX trends. Symbols in panels designate trend significance at the 95% confidence level based on a  $t$ -test. Trend units are  $\text{W m}^{-2} \text{ year}^{-1}$ .



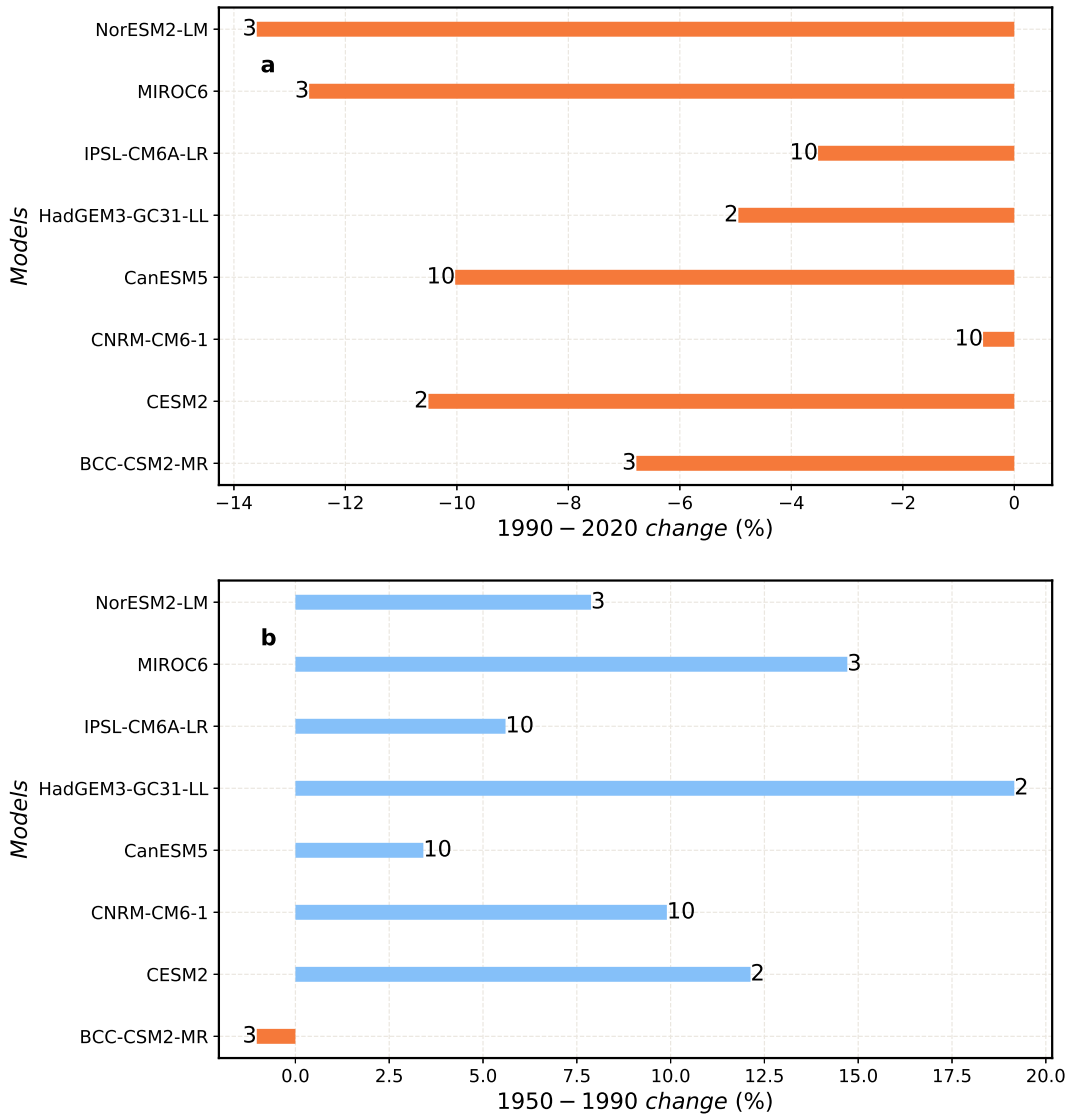
**SUPPLEMENTARY FIGURE 9 Annual mean sea level pressure and surface wind trends in reanalyses.** 1990-2019 (top panels) Modern Era Retrospective-Analysis for Research and Applications version 2 Reanalysis (MERRA2) (a) sea level pressure (PSL) and (b) surface wind speed (SFWD) trends; and (middle panels) European Centre for Medium-Range Weather Forecasts (ECMWF) Reanalyses (ERA5) (c) SLP and (d) SFWD. (bottom panels) 1950-1990 National Center for Environmental Prediction (NCEP) Reanalysis version 1 (e) PSL and (f) SFWD trends. Symbols in panels designate trend significance at the 95% confidence level based on a  $t$ -test. Trend units for PSL and SFWD are  $\text{hPa year}^{-1}$  and  $\text{m s}^{-1} \text{ year}^{-1}$ , respectively.



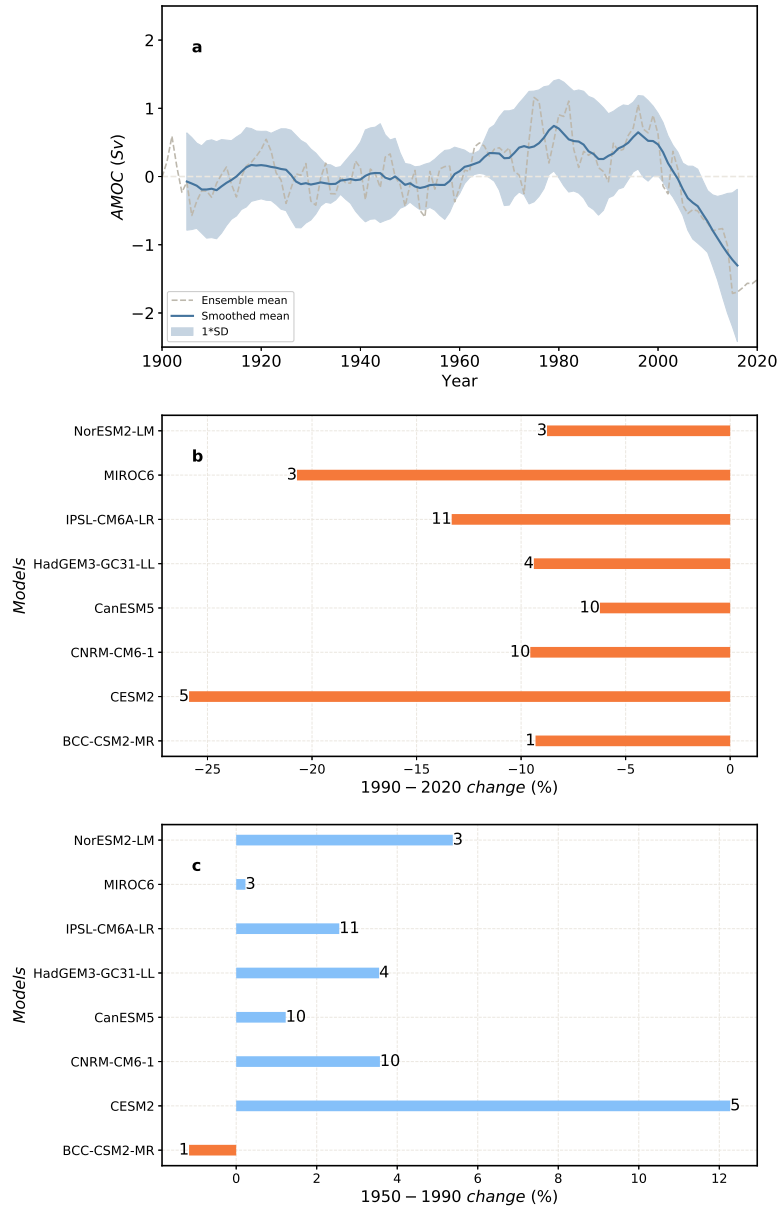
**SUPPLEMENTARY FIGURE 10 1950-1990 annual mean Coupled Model Intercomparison Project phase 6 ensemble mean heat flux decomposition trends.** CMIP6 (left column) all forcing, (middle column) anthropogenic aerosol (AA) forcing, and (right column) greenhouse gas (GHG) forcing ensemble mean trends for the decomposition of (top panels) latent heat flux (LHFLX) into its (a-c) wind and (d-f) moisture components; and (bottom panels) sensible heat flux (SHFLX) into its (g-i) wind and (j-l) temperature components. Symbols designate trend significance at the 95% confidence level based on a *t*-test. Trend units are  $\text{W m}^{-2} \text{ year}^{-1}$ .



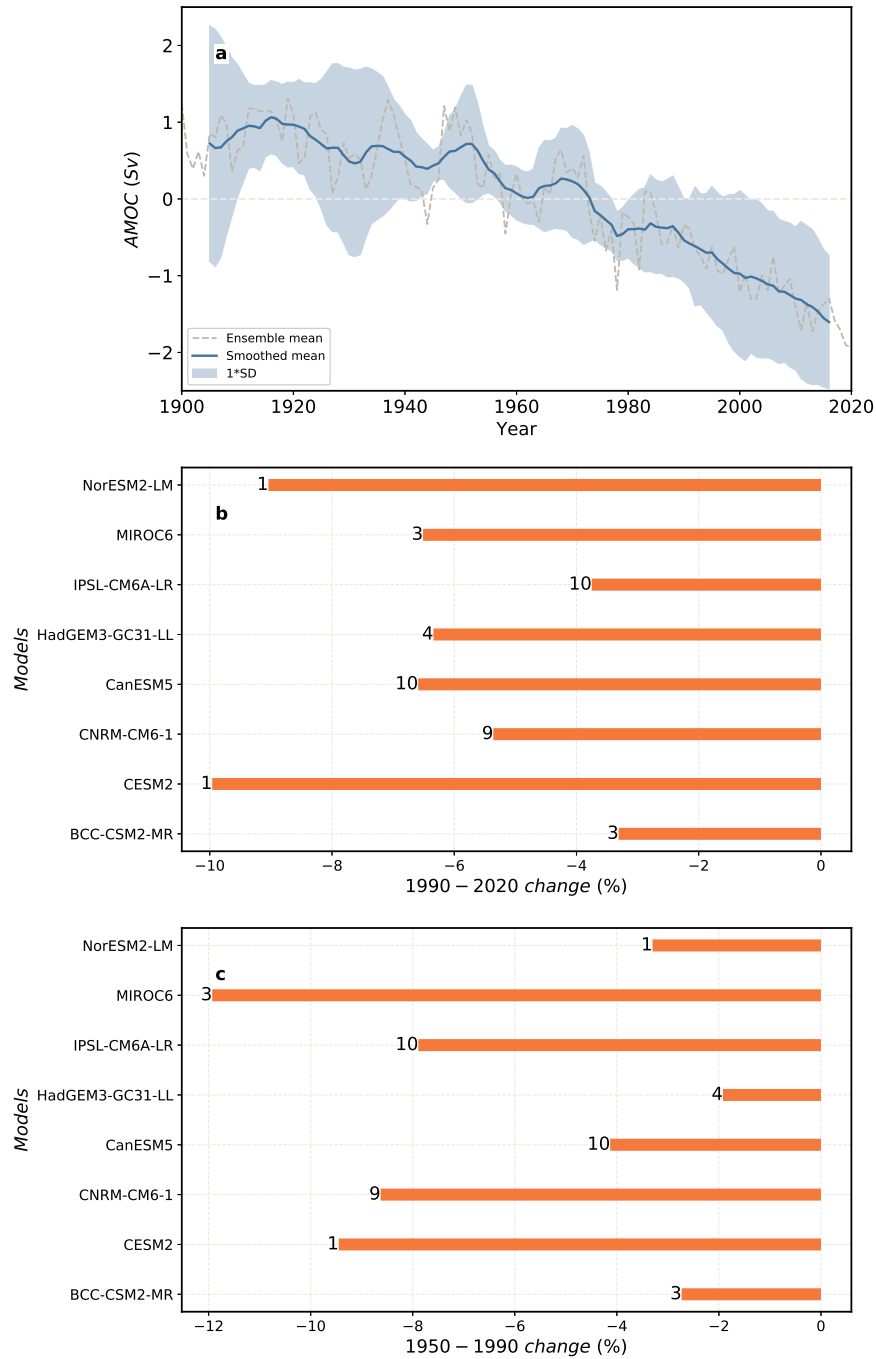
**SUPPLEMENTARY FIGURE 11 1990-2020 annual mean Coupled Model Intercomparison Project phase 6 ensemble mean heat flux decomposition trends.** CMIP6 (left column) all forcing, (middle column) anthropogenic aerosol (AA) forcing, and (right column) greenhouse gas (GHG) forcing ensemble mean trends for the decomposition of (top panels) latent heat flux (LHFLX) into its (a-c) wind and (d-f) moisture components; and (bottom panels) sensible heat flux (SHFLX) into its (g-i) wind and (j-l) temperature components. Symbols designate trend significance at the 95% confidence level based on a *t*-test. Trend units are  $\text{W m}^{-2} \text{ year}^{-1}$ .



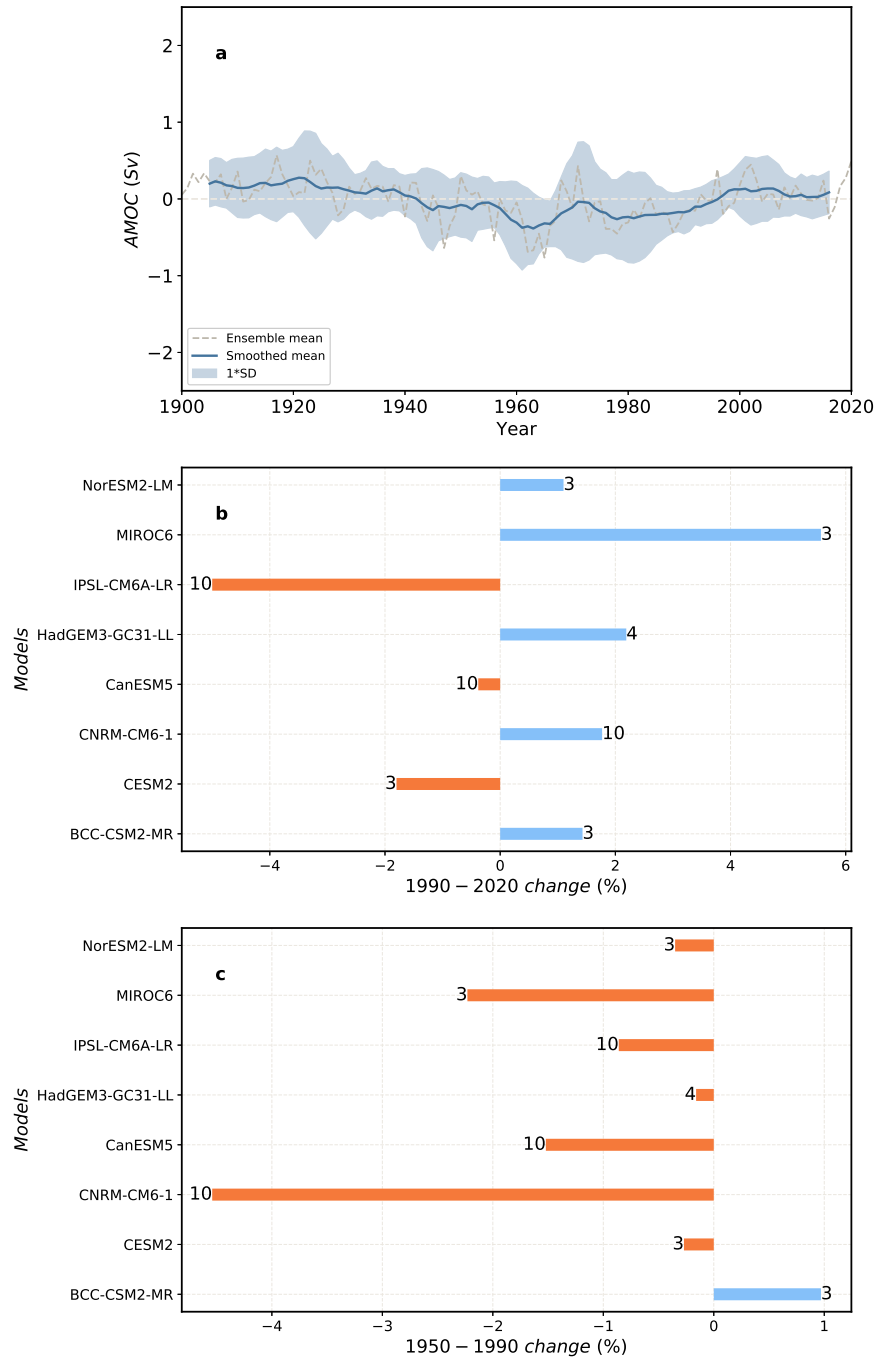
**SUPPLEMENTARY FIGURE 12 Ensemble mean AMOC percent change in anthropogenic aerosol forcing Coupled Model Intercomparison Project phase 6 models.** Ensemble mean (a) 1990-2020 and (b) 1950-1990 AMOC percent change [%] for each model. AMOC weakening (strengthening) is shown with orange (blue) bars. Numbers in front of each bar represent the number of simulations used for that model. The AMOC percent change is estimated from the least-squares regression slope ( $r_s$ ) of the non-normalized AMOC time series using:  $100 \times \frac{r_s \times N}{AMOC(N=1)}$ , where  $N$  is the number of years (e.g., 30 for 1990-2020) and  $AMOC(N=1)$  is the initial AMOC strength (e.g., in 1990 for 1990-2020).



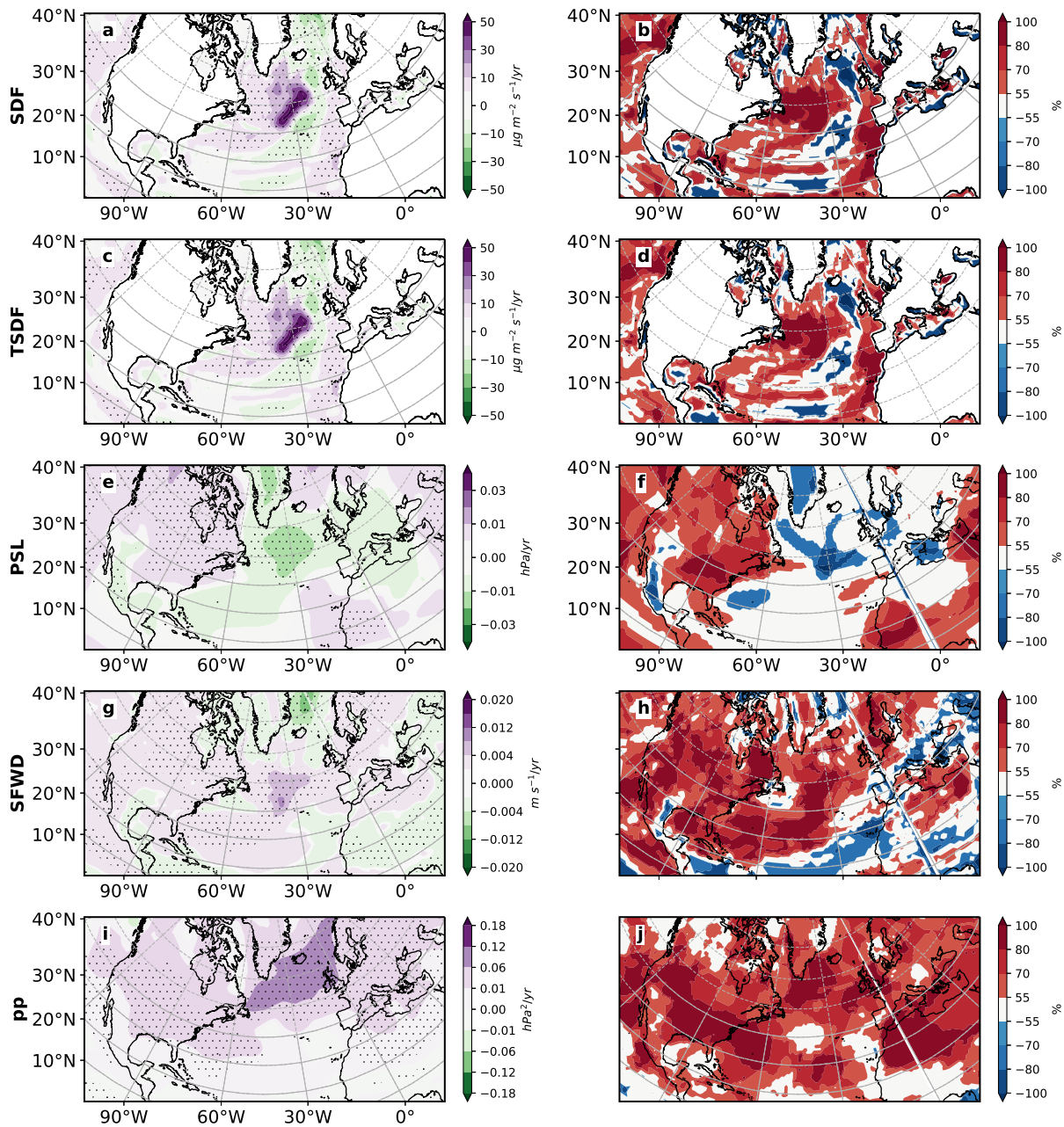
**SUPPLEMENTARY FIGURE 13 Atlantic Meridional Overturning Circulation using the 8 model subset of all forcing Coupled Model Intercomparison Project phase 6 models.** (a) 1900-2020 annual mean ensemble mean AMOC normalized time series. This is based on the same 8 models as are available for the CMIP6 anthropogenic aerosol (and greenhouse gas and natural forcing) simulations. The ensemble mean time series (gray dashed) is smoothed using a 10-year running mean (solid blue line). Shading shows the corresponding inter-model standard deviation. Each model is normalized by its long-term (1900-2020) climatology. Units are Sverdrups (Sv), where 1 Sv is equal to  $10^6 \text{ m}^3 \text{ s}^{-1}$ . Ensemble mean (b) 1990-2020 and (c) 1950-1990 AMOC percent change [%] for each model. AMOC weakening (strengthening) is shown with orange (blue) bars. Numbers in front of each bar represent the number of simulations used for that model. The AMOC percent change is estimated from the least-squares regression slope ( $r_s$ ) of the non-normalized AMOC time series using:  $100 \times \frac{r_s \times N}{AMOC(N=1)}$ , where  $N$  is the number of years (e.g., 30 for 1990-2020) and  $AMOC(N=1)$  is the initial AMOC strength (e.g., in 1990 for 1990-2020).



SUPPLEMENTARY FIGURE 14 **Atlantic Meridional Overturning Circulation in greenhouse gas forcing Coupled Model Intercomparison Project phase 6 models.** (a) 1900-2020 annual mean ensemble mean AMOC normalized time series. The ensemble mean time series (gray dashed) is smoothed using a 10-year running mean (solid blue line). Shading shows the corresponding inter-model standard deviation. Each model is normalized by its long-term (1900-2020) climatology. Units are Sverdrups (Sv), where 1 Sv is equal to  $10^6 \text{ m}^3 \text{ s}^{-1}$ . Ensemble mean (b) 1990-2020 and (c) 1950-1990 AMOC percent change [%] for each model. AMOC weakening (strengthening) is shown with orange (blue) bars. Numbers in front of each bar represent the number of simulations used for that model. The AMOC percent change is estimated from the least-squares regression slope ( $r_s$ ) of the non-normalized AMOC time series using:  $100 \times \frac{r_s \times N}{AMOC(N=1)}$ , where  $N$  is the number of years (e.g., 30 for 1990-2020) and  $AMOC(N=1)$  is the initial AMOC strength (e.g., in 1990 for 1990-2020).



**SUPPLEMENTARY FIGURE 15 Atlantic Meridional Overturning Circulation in natural forcing Coupled Model Intercomparison Project phase 6 models.** (a) 1900-2020 annual mean ensemble mean AMOC normalized time series. The ensemble mean time series (gray dashed) is smoothed using a 10-year running mean (solid blue line). Shading shows the corresponding inter-model standard deviation. Each model is normalized by its long-term (1900-2020) climatology. Units are Sverdrups (Sv), where 1 Sv is equal to  $10^6 \text{ m}^3 \text{ s}^{-1}$ . Ensemble mean (b) 1990-2020 and (c) 1950-1990 AMOC percent change [%] for each model. AMOC weakening (strengthening) is shown with orange (blue) bars. Numbers in front of each bar represent the number of simulations used for that model. The AMOC percent change is estimated from the least-squares regression slope ( $r_s$ ) of the non-normalized AMOC time series using:  $100 \times \frac{r_s \times N}{AMOC(N=1)}$ ,<sup>17</sup> where  $N$  is the number of years (e.g., 30 for 1990-2020) and  $AMOC(N=1)$  is the initial AMOC strength (e.g., in 1990 for 1990-2020).



**SUPPLEMENTARY FIGURE 16 1950-1990 annual mean anthropogenic aerosol forcing Coupled Model Intercomparison Project phase 6 ensemble mean trends and model agreement on the sign of the trend.** (a-b) surface density flux (SDF); (c-d) thermal SDF; (e-f) sea level pressure (PSL); (g-h) surface winds (SFWD); and (i-j) storm track activity (pp). Left panels show the ensemble mean trend; right panels show model agreement on the sign of the trend for each model's ensemble mean. Symbols in left panels designate trend significance at the 95% confidence level based on a  $t$ -test. SDF and TSDf trend units are  $\frac{\mu\text{g}}{\text{m}^2\text{-s}} \text{ year}^{-1}$ . PSL, pp, and SFWD trend units are  $\text{hPa year}^{-1}$ ,  $\text{hPa}^2 \text{ year}^{-1}$ , and  $\text{m s}^{-1} \text{ year}^{-1}$ , respectively. Trend realization agreement units are %. Red (blue) colors indicate model agreement on a positive (negative) trend.